EPJ Web of Conferences **205**, 02020 (2019) https://doi.org/10.1051/epjconf/201920502020
*UP 2018*

# Femtosecond XUV induced dynamics of the methyl iodide cation

*Geert* Reitsma[1,¯], *Marta L.* Murillo-Sánchez[2] , *Rebeca* de Nalda[3], *Mariu E.* Corrales[2], *Sonia* Marggi Poullain[2,4], *Jesús* González-Vázquez[4,5], *Marc J.J.* Vrakking[1], *Luis* Bañares[2] and *Oleg* Kornilov[1]

[1]Max Born Institute for Nonlinear Optics and Short Pulse Spectroscopy, Max-Born-Strasse 2A, 12489 Berlin, Germany.
[2]Departamento de Química Física (Unidad Asociada I+D+i al CSIC), Facultad de Ciencias Químicas, Universidad Complutense de Madrid, 28040 Madrid, Spain.
[3]Institito de Química Física Rocasolano, CSIC, C/Serrano 119, E-28006 Madrid, Spain.
[4]Departamento de Química, Facultad de Ciencias, Universidad Autónoma de Madrid, Módulo 13, 28049 Madrid, Spain.
[5]Institute for Advanced Research in Chemical Sciences (IAdChem), Faculdad de Ciencias, Universidad Autónoma de Madrid, 28049, Spain.

**Abstract.** Ultrashort XUV wavelength-selected pulses obtained with high harmonic generation are used to study the dynamics of molecular cations with state-to-state resolution. We demonstrate this by XUV pump - IR probe experiments on $CH_3I^+$ cations and identify both resonant and non-resonant dynamics.

## 1 Introduction

Ultrashort extreme ultraviolet (XUV) pulses obtained from high harmonic generation (HHG) allow for studies of the dynamics in molecular cations. Typical pump-probe experiments using HHG have excellent time-resolution and can access processes such as charge migration [1], evolution of electronic and vibrational wavepackets [2], and fast decays through conical intersections [3]. However, in experiments using the full bandwidth of HHG sources, signals from different states are often mixed, which makes interpretation difficult. Here, we employ a time-delay-compensating XUV monochromator [4] which defines the photon energy and allows to study the state-to-state dynamics and also to distinguish processes in cations from those in highly excited neutrals, because the former are present with all harmonics of sufficient energy and the latter are resonant and thus only present for a certain XUV photon energy. The monochromator delivers selected harmonics, obtained from the output of an HHG-source, with a spectral bandwidth of 300 meV and a time duration of 20-25 fs. To perform pump-probe experiments, the wavelength-selected XUV beam is recombined with 25 fs IR pulses. In the present contribution we investigate the dynamics of cationic states of the $CH_3I$ molecule. The dissociation of the $CH_3I^+$ cation along the C-I axis is mainly accompanied by a geometry change in the methyl part from

¯ Corresponding author: reitsma@mbi-berlin.de

pyramid to planar and the spin-orbit splitting in the iodine atoms [5]. The latter induces avoided crossings in the manifold of potential energy surfaces which make $CH_3I^+$ dissociation complex and interesting.

## 2 Results and Discussion

In the experiments, we used three harmonics: the 7th, 9th, and 11th of the 800 nm fundamental driving pulse. With photon energy $E_{ph}$ = 10.9 eV (7th harmonic), only the spin-orbit split ground state ( $\tilde{X}\ ^2E_{3/2,1/2}$) can be populated. With the next harmonic $E_{ph}$ = 14.0 eV (9th harmonic), the weakly bound first excited state ( $\tilde{A}\ ^2A_1$) is populated as well, while the 11th harmonic ($E_{ph}$ = 17.1 eV) also reaches the repulsive $\tilde{B}\ ^2E$ state. Note that at these photon energies also neutral Rydberg series converging to the respective excited cations can be resonantly excited, leading to fluorescence, auto-ionization, or neutral dissociation processes. For each harmonic we record ion velocity map images for both the $CH_3I^+$ and $I^+$ fragments, observing both dynamics in the cation as well as dynamics of resonant neutral states.

With $E_{ph}$ = 10.9 eV photons, no decay dynamics in the cation are expected upon ionization to the $\tilde{X}\ ^2E_{3/2,1/2}$ spin-orbit ground states since both states are bound and their vibrational activity is negligible [6]. However, in the experiment we observe an enhancement of the signal at temporal overlap followed by a decay with a time constant of 90fs. This behavior cannot be explained by cation dynamics, and therefore must come from dynamics in the neutral molecule upon resonant absorption. This is supported by the fact that these dynamics are not observed for higher harmonics. Previous photoabsorption studies indeed have identified Rydberg series converging to the $\tilde{A}\ ^2A_1$ and $\tilde{B}\ ^2E$ potential energy surfaces [7]. Calculations are currently in progress to establish with certainty which of these states are responsible for the observed behavior and to explain the observed 90 fs decay timescale.

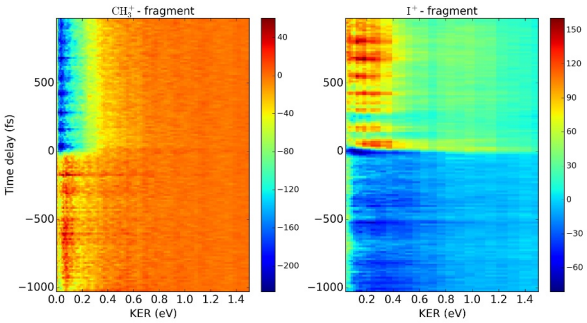


**Fig 1.** Time-dependent kinetic energy release maps of the $CH_3^+$ (a) and $I^+$ (b) obtained with a 17.1 eV XUV pump pulse and an IR probe pulse. A positive delay means that the IR pulse comes after the XUV pulse.

For photon energies of 14.0 and 17.1 eV we obtain very comparable data, both different from 10.9 eV. Figure 1 displays maps of the total kinetic energy release (KER) as a function of time delay for dissociation into $I + CH_3^+$ and $CH_3 + I^+$, obtained for the $E_{ph}$ = 17.1 eV pump and IR probe scheme. When IR comes after XUV, the yield of $CH_3^+$ fragments decreases while the yield of $I^+$ fragments is enhanced. On top of this long-lived contribution, clear oscillatory signals are observed in both ionic fragment yields. The period of this oscillation is 127 ± 3 fs and the oscillations in the $CH_3^+$ and $I^+$ yield are in opposite phase with respect to each other.

The observed frequency closely corresponds to the frequency of the C-I stretching mode in the $\tilde{A}\ ^2A_1$ state [8]. Therefore we interpret the observation as follows. The $\tilde{A}\ ^2A_1$ state is populated at the inner turning point of the potential well, launching a wavepacket composed of several vibrational states. In the XUV-only experiment the most common dissociation pathway would be a non-adiabatic coupling to hot vibrational bands in the spin-orbit split ground state of the cation $\tilde{X}\ ^2E_{3/2,1/2}$. The molecule then statistically dissociates producing $CH_3^+$. The latter mechanism is consistent with the discrepancy between lifetime of the $\tilde{A}\ ^2A_1$ state ($10^{-10}$ s) and the dissociation rate constant ($10^{-7}$ s) [8,9]. The low total KER for the dissociation into $I + CH_3^+$ is also consistent with this scenario.

The IR pulse couples the $\tilde{A}\ ^2A_1$ state population to a repulsive potential energy surface leading to dissociation into $CH_3 + I^+$. As this state serves as a common final state for the coherently populated vibrational levels in the $\tilde{A}\ ^2A_1$ state, these pathways interfere with a beating frequency equivalent to the energetic separation between those states. The fact that dissociation into $CH_3 + I^+$ occurs with a nonzero KER indicates a prompt dissociation process. Inherently, the $I + CH_3^+$ dissociation channel should exhibit the same oscillation, but with opposite sign.

To complete the picture, it is necessary to know the exact probing mechanism induced by the IR. The potential energy surfaces of reference [5] can qualitatively describe the probing step. Further calculations are underway to obtain further insight into the role of the IR field on the coupling to dissociative states.

## 3 Conclusion

We used ultrafast wavelength-selected XUV pulses to study the dynamics of the lowest excited electronic states of the $CH_3I^+$ cation. We observed dynamics upon resonant absorption by members of Rydberg series converging to these ion states as well as vibrational wavepacket dynamics that can be used to steer the dissociation to either the $I + CH_3^+$ or the $CH_3 + I^+$ channels depending on the phase of the wavepacket at the arrival time of the probe pulse. In the future, we aim to quantify this control process with the help of potential energy surface calculations on which a wavepacket will be propagated in the presence of the IR field.

This work has been supported by Laser lab Europe.

## References

[1] F. Calegari, D. Ayuso, A. Trabattoni, et al, Science **346**, 336-339 (2014).
[2] F. Kelkensberg, C. Lefebvre,W. Siu, et al, Phys. Rev. Lett. **103**, 123005 (2009).
[3] M. C. E. Galbraith, S. Scheit, N. V. Golubev, et al, Nature Communications. **8**, 1018 (2017).
[4] M. Eckstein, C.-H. Yang, M. Kubin, et al, J. Phys. Chem. Lett. **6**, 419–425 (2015).
[5] S. Marggi Poullain, D. V. Chicharro, J. Gonzalez-Vazquez, et al, Phys. Chem. Chem. Phys. **19**, 7886–7896 (2017).
[6] L. Karlsson, R. Jadrny, L. Mattsson, et al, Phys. Scr. **16**, 225–234 (1977).
[7] R. Locht, B. Leyh, H. W. Jochims, et al, Chem. Phys. **365**, 109–128 (2009).
[8] S. Goss, D. Mcgilvery, J. Morrison et al, J. Chem. Phys. **75**, 1820–1828 (1981).
[9] D. Mintz and T. Baer, J. Chem. Phys. **65**, 2407–2415 (1976).